Elemental bio-imaging of trace elements in teeth using laser ablation-inductively coupled plasma-mass spectrometry

Introduction

There is increasing recognition of the role of trace elements in oral health. A large body of evidence supports the caries-protective role of fluoride (1), and more recent reports have implicated Pb and Cd with the formation of dental caries (2, 3) and periodontal disease (4). Other trace metals such as Zn, Cu, Fe, Se, Sn and Al in tooth enamel may also play a role in dental caries but the role of these elements is not clear (5, 6). Teeth not only serve as targets for the effects of metal exposure but have also been used as bio-indicators of environmental exposure to metals, infant nutrition and disease outcomes (7). Pb levels in primary teeth are a well-established indicator of environmental Pb exposure in children and adolescents, and have been linked to several neuro-developmental health outcomes (8). However, a majority of such studies have used whole teeth or fragments of dentine to estimate environmental exposure to metals and subsequent health effects. A major barrier to the detailed study of metal uptake in teeth and the further development of tooth-metal concentrations as a time-specific biomarker of environmental exposure has been the absence of readily accessible analytical methods that can reliably measure the spatial distribution of metals in teeth.

Current methods for the spatial analysis of teeth using element-specific detection include synchrotron microprobe x-ray fluorescence (SXRF) (9-11), particle-induced x-ray emission (PIXE) (12-16), and secondary ion mass spectrometry (SIMS) (17). However, these methods are expensive, which prohibits their use in large epidemiologic studies. Teeth have also been acid digested and analyzed by atomic absorption spectroscopy (AAS) (18), inductively coupled plasma-optical emission spectroscopy (ICP-OES) and inductively coupled plasma -mass spectrometry (ICP-MS) (7, 19). .

Elemental bio-imaging employing laser ablation-inductively coupled plasma-mass spectrometry (LA-ICP-MS) is a new method for imaging trace elements in biological tissues (20). Our laboratory has applied this technique to the imaging of trace elements in mouse brains (21), osteoarthritic joints (22) and human lymphatic tissues (23, 24). LA-ICP-MS is a relatively simple technique that does not require a high vacuum ion source or suffer from severe matrix effects. Complicated and often hazardous digestion procedures are not required as it is a solid-state analyzer. Additionally, the lower spatial resolution compared to PIXE (0.1-10 μm) is better suited to imaging the entire tooth. LA-ICP-MS applications have been limited to spot ablation and small area rastering to determine approximate spatial distribution of trace elements in teeth (25, 26). Detailed elemental maps of entire tooth sections using LA-ICP-MS have not previously been reported. In this paper we apply this novel method for quantitative imaging of trace elements in teeth. This preliminary study demonstrates the potential for using LA-ICP-MS imaging in studying tooth microchemistry and monitoring trace elements concentrations, including important developmental nutrients and environmental toxicants.

Materials and methods

Sample Preparation

Naturally shed deciduous incisors collected from children living in a rural community of Australia were analyzed. These teeth were part of a larger sample set examining the impact of trace element distribution in dental development. Three incisors that were free of dental caries, any obvious developmental defects, and also histologically unremarkable, (samples BH3, BH4 and BH10) were selected for analysis. Written consent was obtained from the parents/guardians of the participants. Ethics approval for this study was obtained from the Human Research Ethics Committee of the Far Western Area Health Service, New South Wales, Australia.

At the time of collection, teeth were washed in distilled water, air-dried and placed individually in sterile plastic specimen containers (Sarstedt, Australia). The participant's name, type of tooth, and date of exfoliation were noted on the container and forwarded to the laboratory. Teeth were subsequently washed in an ultrasonic bath of 18 MΩcm water, dried and embedded in resin at 70 °C

for 10 h (Taab Laboratories Equipment Inc. Berkshire, UK). Embedded teeth were sectioned using a rotary stainless-steel blade (Leitz-1600, Germany) in a vertical plane that passed through the cusp tip. The incisors were sectioned in the labio-lingual plane. Prior to analysis, samples were cleaned in an ultrasonic bath of ultrafiltered deionized water and dried in an oven at 60 °C for 2 h.

Laser ablation-inductively coupled plasma-mass spectrometry

The laser ablation unit used was a New Wave Research UP-213 system (Kennelec Technologies, Mitcham, Victoria, Australia) equipped with a Nd:YAG laser emitting a nanosecond laser pulse in the fifth harmonic with a wavelength of 213 nm. The standard ablation cell was replaced with a Large Format Cell (LFC). The LFC has a large volume chamber capable of holding samples up to 15.2 cm^2 in area. The *x-y-z* stage of the LFC employs a small volume 'roving' sampling cup that traverses the sample while the laser beam remains stationary.

An approximately 40 cm length of Tygon® tubing (i.d. 3 mm) connected the laser ablation unit to an Agilent Technologies 7500cx (Agilent Technologies Australia, Forrest Hill, Victoria, Australia) ICP-MS. The instrument was fitted with a 'cs' lens system for enhanced sensitivity.

The system was tuned daily for sensitivity using National Institute of Standards and Technology (NIST) Standard Reference Material (SRM) 612 Trace elements in glass. Polyatomic oxide interference was evaluated and minimized by monitoring the Th^+/ThO^+ (m/z 232/248) ratio. Typical oxide formation was consistently under 0.3 %. Operating conditions for the optimized LA-ICP-MS system are given in Table 1. Variable parameters included plasma power, argon gas flow rates, sample depth (and thereby residence time of analytes in the plasma), lens voltages for ion beam focusing and integration times for the mass spectrometer.

Table 1: Typical operating conditions for LA-ICP-MS system.

Agilent 7500ce ICP-MS		**New Wave UP213 Laser Ablation**	
RF power	1250 W	Wavelength	213 nm
Plasma gas flow rate	15 L min^{-1}	Repetition frequency	20 Hz
Carrier gas flow rate	1.15-1.25 L min^{-1}	Laser energy density	1 J cm^{-2}
Sample depth	4.0 mm	Spot size	30 µm
Quadrupole bias	-5 V	Scan rate	30 µm s^{-1}
Octopole bias	-8 V	Line spacing	30 µm
Scan mode	Peak hopping	Carrier gas	Ar
Dwell time	0.1 s per m/z		
Measured m/z	31, 44, 66, 88, 111, 208		
Extracts 1, 2	6.8, -126 V		

Standard reference material (SRM) analysis

Approximately 1 g of NIST SRM 1486 bone meal was pressed into a high-density pellet using a KBr press. Prior to the analysis of each sample 7 representative lines of ablation were made of the NIST SRM 1486 standard. Identical ablation conditions were used for standard and sample analysis. NIST SRM 1486 was selected as an appropriate standard for the quantification of trace elements in teeth due to the major component being crude hydroxyapatite. Suitability of NIST SRM 1486 was confirmed by direct comparison of mean $^{44}Ca/^{31}P$ ratios in both the standard (1.14) and each sample (range: 1.05-1.25). Certified concentrations of NIST SRM 1486 are given in Table 2. The Cd concentration was indicated by…?

Table 2: Certified concentrations of trace elements in NIST SRM 1486 Bone meal **concentration not certified*

Element	**Certified concentration (% w/w)**	**Element**	**Certified concentration (µg g^{-1})**
Calcium	26.58 ± 0.24	Lead	1.335 ± 0.014
Phosphorus	12.30 ± 0.19	Strontium	264 ± 7
		Zinc	147 ± 16

		Cadmium	0.003*

Image processing

Each line of ablation produced a single data file in comma separated value (.csv) format. Data was processed using Interactive Spectral Imaging Data Analysis Software (ISIDAS), a custom-built software tool written using Python programming language. ISIDAS reduces all .csv files into a single, exportable visualization toolkit (.vtk) file format. Images were not normalised to an 'internal standard' measured mass, as the only suitable element present at % w/w concentrations (Ca) has been shown to vary significantly in distribution across the three major regions of the tooth (27) Images were produced by exporting .vtk files into MayaVi2 (Enthought Inc., Austin, Texas, USA), an open source data visualization application. Quantitative data recorded by the ablation of a representative area of NIST SRM 1486 was used to produce a single point calibration (plus gas blank), allowing for conversion of counts per second to concentration values by simple linear regression of the certified value against the mean signal intensity for *n* = >300 data points.

Results

Figure 1 shows a sample image created using the single-point calibration LA-ICP-MS method described. A 30 μm diameter laser beam was used for all experiments, traversing the sample at a rate of 30 μm s^{-1}. Ablation lines were spaced precisely 30 μm apart. Integration parameters for the MS were set so as to acquire one data point per second for each measured mass. Consequently, each pixel represents the signal intensity corresponding to a 30 μm^2 area of ablation. These values were converted to concentration (μg g^{-1} or ng g^{-1}) according to the response from ablation of the NIST SRM 1486 (bone meal) standard and a measured gas blank. Corresponding concentration vs distance (in mm) plots are also shown in both the *x* and *y*-axes. Errors in quantitative measurements varied between isotopes, from 12.0 % for ^{208}Pb to 41.2 % for ^{111}Cd. The bone meal standard is manufactured by sieving through a 355 μm mesh (28), and our procedure of compression into a pellet does not ensure homogeneity. This limits our ability to quantify the trace element concentrations as the bone meal standard is heterogeneous at the sampling resolution used in our LA-ICP-MS analyses (30 μm).

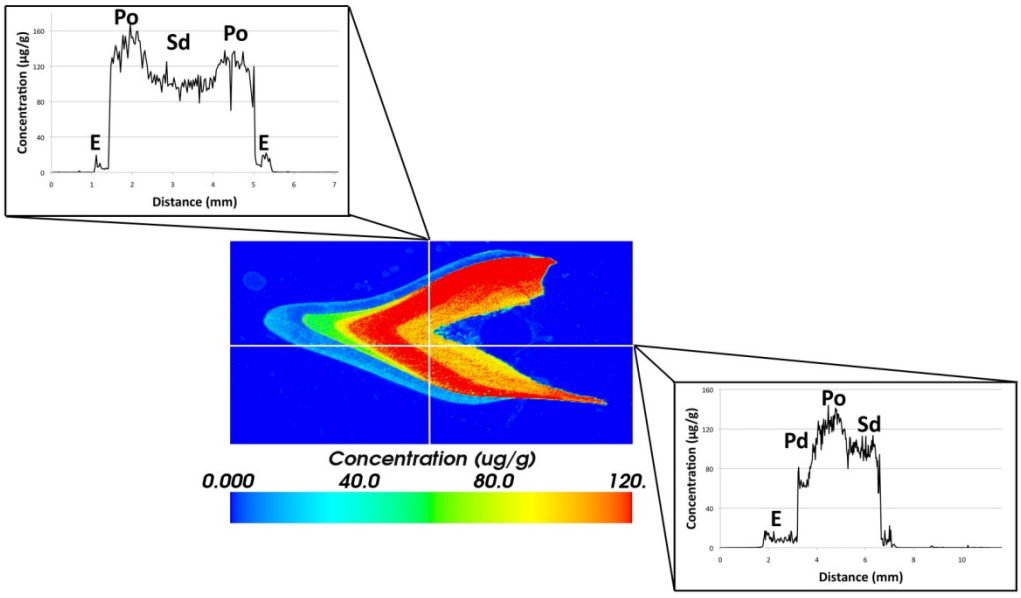

Figure 1: Two-dimensional concentration vs distance plots for horizontal and vertical lines in ^{88}Sr image. Enamel (E), prenatal dentine (Pd), postnatal dentine (Po) and secondary dentine (Sd) are shown on the horizontal and vertical line plots.

Figure 2 shows quantitative element maps of several trace elements in tooth BH3. Images from teeth BH10 and BH4 are shown in Figure 3 and Figure 4, respectively. Sr was observed at concentrations over 120 ± 31 μg g^{-1} in all teeth, with notably higher concentrations present in the dentine approaching the pulp cavity. Distinct features were observed in the Sr map of tooth BH3 (Figure 3). Sr concentrations in enamel (E) were markedly lower than in dentine. Furthermore, prenatal dentine (Pd) showed lower levels than postnatal dentine (Po). There was also a distinct variation in the Sr concentrations in the dentine formed immediately after birth which is seen as a yellow coloured zone, corresponding to a Sr concentration of approximately 90 ± 23 μg g^{-1}. The concentrations of Sr rose to approximately 120-160 (± 31-41) μg g^{-1} in the postnatal primary dentine and then declined in the region of the secondary dentine (Sd) immediately adjacent the pulp chamber.

Maximum Zn concentrations in the three teeth varied from 250 ± 55 to 750 ± 165 μg g^{-1}. In all teeth, Zn concentrations in enamel were lower than in dentine. Within the enamel, the highest Zn levels were seen at the outer edge with the inner enamel having very low concentrations (< 10 ± 2 μg g^{-1}). In dentine, Zn was concentrated at the dentine-pulp margin and in the cervical dentine. Accumulation of the heavy metals Pb and Cd (in two of three samples) was also observed in the 0-30 ng g^{-1} and 0-300 ng g^{-1} range, respectively, with higher levels at the dentine-pulp margin.

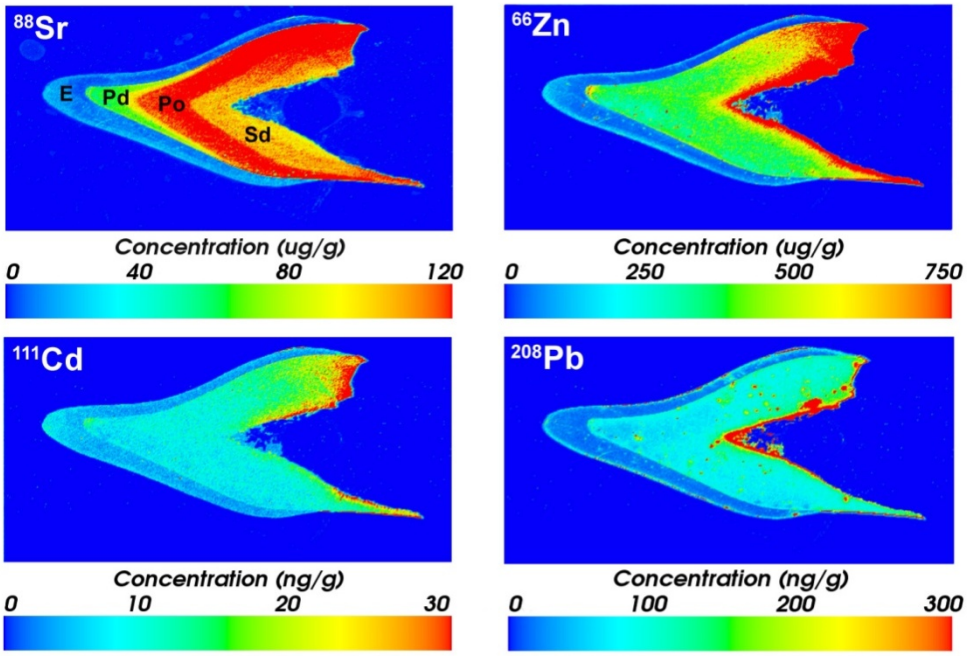

Figure 2: Elemental images of ^{88}Sr, ^{66}Zn (μg g^{-1}), ^{111}Cd and ^{208}Pb (ng g^{-1}) in tooth BH3. Quantitative information is based on a single-point calibration. In the ^{88}Sr map, enamel (E), prenatal dentine (Pd), postnatal dentine (Po) and secondary dentine (Sd) are shown.

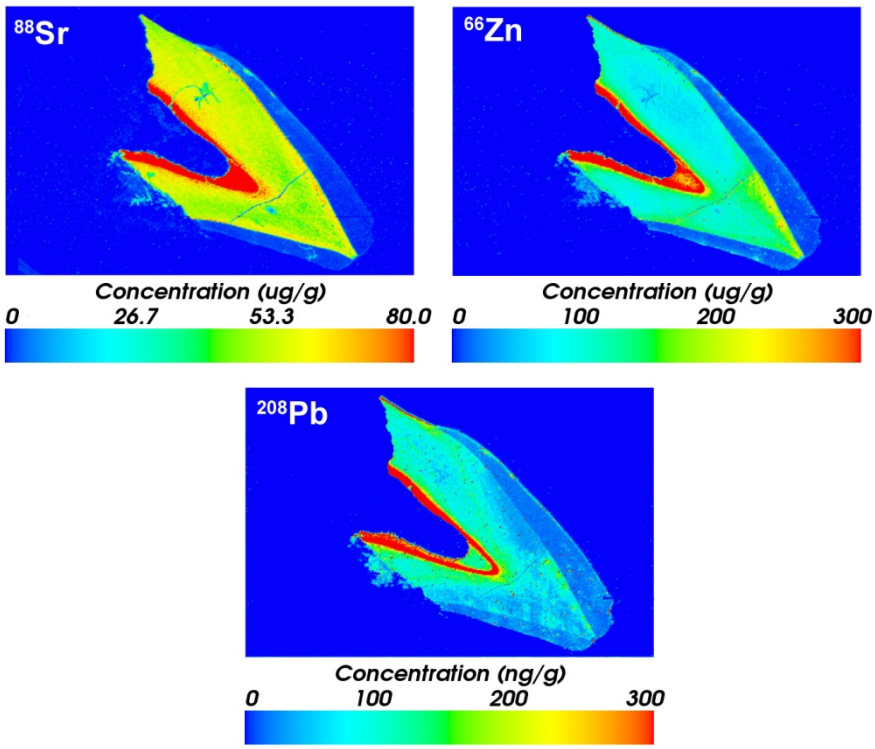

Figure 3: Elemental images of ^{88}Sr, ^{66}Zn ($\mu g\ g^{-1}$) and ^{208}Pb (ng g^{-1}) in tooth BH10. Quantitative information is based on a single-point calibration.

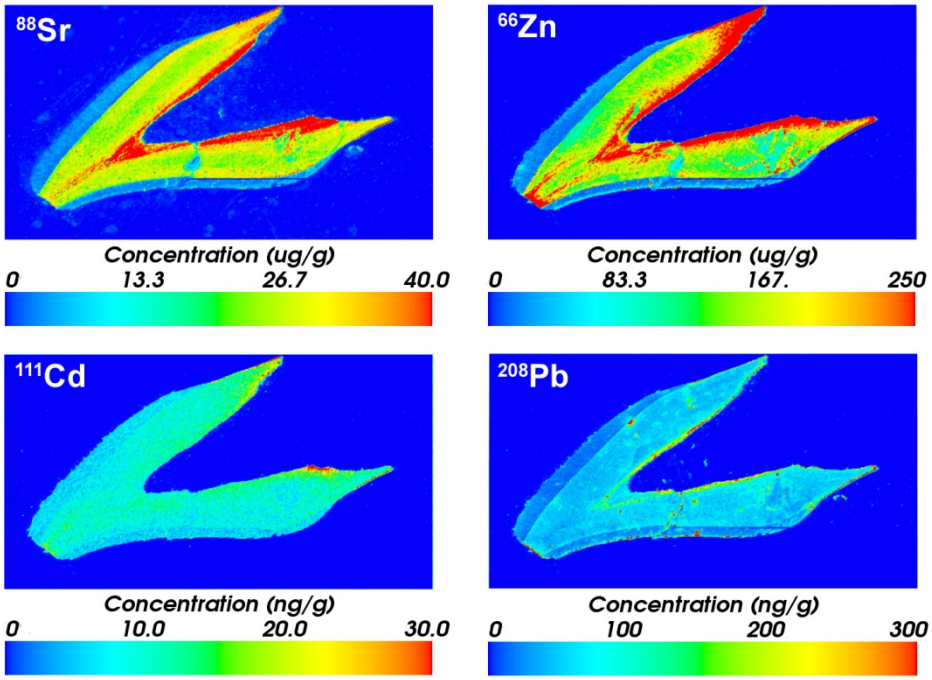

Figure 4: Elemental images of ^{88}Sr, ^{66}Zn ($\mu g\ g^{-1}$), ^{111}Cd and ^{208}Pb (ng g^{-1}) in tooth BH4. Quantitative information is based on a single-point calibration.

Discussion

Sr was observed at concentrations over 120 μg g^{-1} in all teeth, with notably higher concentrations present in the dentine approaching the pulp cavity. Zaichick *et al.* reviewed 20 publications that determined the Sr content in the enamel of intact permanent human teeth and found the measured range of Sr in these reports was from 50 to 318 μg g^{-1} (29). Sr concentrations exhibit heterogeneity throughout the tooth structure, and environmental exposures have been implicated as a major factor in this variation (with concentrations up to 1363 μg g^{-1} in subjects exposed to Sr-rich foods) (10). The higher concentrations of Sr in dentine formed immediately after birth in tooth BH3 (Figure 2) may be related to intake of infant formulas (which are known to have high concentrations of Sr) (30), although this could not be confirmed as dietary histories were not available from the participants.

The concentration of Zn in the samples agreed with previously reported studies of Zn in primary teeth (31). However, these results contrast those reported by Brown *et al. (ref)*, who reported that in a sample of teeth analysed by acid digestion and ICP-MS and ICP-OES the concentration of Zn was evenly distributed throughout the enamel and dentine. This further illustrates the advantages of spatial elemental maps over measurements taken in digested samples or even single-point/small region LA-ICP-MS analyses. Variation between enamel and dentine Pb concentrations observed previously were confirmed (32, 33). The measured concentration range for Pb fell within that previously reported for lead-exposed children, (40-5600 ng g^{-1}), albeit at the lower end,.

Cd was observed at lower concentrations than those of other elements (ng g^{-1} vs μg g^{-1}), presumably due to the lower affinity of Cd for calcified tissues. Cd was not detected in tooth BH10. Concentrations of Cd in teeth BH3 and BH4 were markedly lower than other recent studies (34). This was likely due to the low exposure to Cd in the rural community where the participants resided, further suggesting that Cd concentrations in teeth, although low, are most likely governed by environmental exposure.

The method offers a number of advantages over other commonly used methods of trace element determination in biological media. Unlike previous LA-ICP-MS methods that employed small area analysis, this imaging procedure provided detailed correlation of metal distribution with histological features at micrometer scale. Further development of the ISIDAS software suite (UTS, Sydney, Australia) will directly align high-resolution digital microscopic methods with elemental images. This method can also potentially be used to reveal more information about metal uptake in teeth, which has significant implications for the study of environmental exposure. In future our laboratory will apply this method to the study of cellular metal transport during tooth development.

The elemental detection limits compare favourably with other methods including energy dispersive x-ray analysis, SIMS, PIXE and SXRF. However, these other methods are capable of 1 μm or better spatial resolution, which is currently not possible with the instrumentation used in the present study. The other major limitation of this technique is the lack of certified analytical standards for comprehensive quantification and method validation. NIST 1486 bone meal is one of the few hydroxyapatite-based standards for trace elements available. NIST 612 Trace elements in glass (ca. 50 mg kg^{-1}) was considered as an additional calibration standard, and was evaluated by comparing percentage recoveries of Mn:Ca ratios in both NIST 1486 and 612 against NIST 610 Trace elements in glass (ca. 500 mg kg^{-1}). NIST 612 showed a mean 1.8 ± 2.7% (*n* = 8) recovery for the certified Mn:Ca ratio when measured using NIST 610 as a reference, whereas NIST 1486 gave a recovery of 22.8 ± 13.1% (*n* = 8) against the same standard. Both NIST 612 and 6120 are Si-based matrices (as SiO_2), compared to Ca-based hydroxyapatite in NIST 1486. It was concluded that the significant variation in chemical composition of the sample matrix prevented the use of NIST 610 and 612 as calibration standards for teeth (35).

Development of synthetic teeth standards homogenous at the μm scale is currently being undertaken in our laboratories. Regardless, application of NIST 1486 bone meal standard in single-point calibration studies by LA-ICP-MS suggested a general accuracy of around ± 20 %, allowing inter-sample trends to be easily identified. The measured maximum concentrations for each element analysed across all teeth fell within the upper calibration range using NIST 1468, with the exception of Zn.

The technique presented here is ideal for quantitatively imaging cross sections of entire teeth in a reasonable timeframe of approximately 12 hours using a single standard. LA-ICP-MS methods can also be applied in the study of metal isotopes revealing not only the intensity but also the sources of metal exposures in at-risk communities.

Conclusions

LA-ICP-MS imaging is a powerful tool for mapping the spatial distribution of trace elements in teeth. Preliminary results indicate that quantitative data can be recoded through the ablation of an appropriate matrix-matched standard, such as NIST SRM 1486 Bone meal. Clear demarcation of trace element deposition in regions of teeth associated with developmental periods were observed for Sr, Zn and Pb. Concentration ranges (ng g^{-1} for Cd and Pb, $\mu g\ g^{-1}$ for Sr and Zn) were consistent with previously reported studies. Elemental bio-imaging has potential to further study the uptake of trace elements during tooth development and their effect on dental health, including the formation of caries, and also for using teeth as trace element biomarkers in environmental biomonitoring studies.

References

1. Marinho VCC, Higgins JPT, Logan S, Sheiham A. Systematic review of controlled trials on the effectiveness of fluoride gels for the prevention of dental caries in children. *Journal of Dental Education* 2003;**67**(4):448-58.
2. Moss ME, Lanphear BP, Auinger P. Association of dental caries and blood lead levels. *Jama-Journal of the American Medical Association* 1999;**281**(24):2294-98.
3. Arora M, Weuve J, Schwartz J, Wright RO. Association of environmental cadmium exposure with pediatric dental caries. *Environmental Health Perspectives* 2008;**116**(6):821-25.
4. Arora M, Weuve J, Schwartz J, Wright RO. Association of Environmental Cadmium Exposure with Periodontal Disease in US Adults. *Environmental Health Perspectives* 2009;**117**(5):739-44.
5. Little MF, Steadman LT. Chemical and physical properties of altered and sound enamel--IV: Trace element composition. *Archives of Oral Biology* 1966;**11**(3):273-78, IN1.
6. Curzon MEJ, Crocker DC. Relationships of trace elements in human tooth enamel to dental caries. *Archives of Oral Biology* 1978;**23**(8):647-53.
7. Brown CJ, Chenery SRN, Smith B, Mason C, Tomkins A, Roberts GJ, Sserunjogi L, Tiberindwa JV. Environmental influences on the trace element content of teeth - implications for disease and nutritional status. *Archives of Oral Biology* 2004;**49**(9):705-17.
8. Needleman HL, Schell A, Bellinger D, Leviton A, Allred EN. The long-term effects of exposure to low-doses of lead in childhood - an 11-year follow-up report. *New England Journal of Medicine* 1990;**322**(2):83-88.
9. Marques AF, Marques JP, Casaca C, Carvalho ML. X-ray microprobe synchroton radiation X-ray fluorescence application on human teeth of renal insufficiency patients. *Spectrochimica Acta Part B: Atomic Spectroscopy* 2004;**59**(10-11):1675-80.
10. Pinheiro T, Carvalho ML, Casaca C, Barreiros MA, Cunha AS, Chevallier P. Microprobe analysis of teeth by synchrotron radiation: environmental contamination. *Nuclear Instruments and Methods in Physics Research Section B: Beam Interactions with Materials and Atoms* 1999;**158**(1-4):393-98.
11. Carvalho ML, Marques AF, Marques JP, Casaca C. Evaluation of the diffusion of Mn, Fe, Ba and Pb in Middle Ages human teeth by synchrotron microprobe X-ray fluorescence. *Spectrochimica Acta Part B: Atomic Spectroscopy* 2007;**62**(6-7):702-06.
12. Svalbe ID, Chaudhri MA, Traxel K, Ender C, Mandel A. Surface profiling of trace elements across pre-carious lesions in teeth. *Nuclear Instruments and Methods in Physics Research Section B: Beam Interactions with Materials and Atoms* 1984;**3**(1-3):651-53.
13. Lane DW, Duffy CA. The analysis of trace elements in human teeth collected from the Oxfordshire area in the UK. *Nuclear Instruments and Methods in Physics Research Section B: Beam Interactions with Materials and Atoms* 1996;**118**(1-4):392-95.

14. Cohen DD, Clayton E, Ainsworth T. Preliminary investigations of trace element concentrations in human teeth. *Nuclear Instruments and Methods in Physics Research* 1981;**188**(1):203-09.
15. Pineda-Vargas CA, Naidoo S, Eisa MEM. Nuclear microanalysis of tooth enamel from a community in the Western Cape, South Africa. *Nuclear Instruments and Methods in Physics Research Section B: Beam Interactions with Materials and Atoms* 2007;**260**(1):190-93.
16. Anwar Chaudhri M, Crawford A. The influence of trace elements of fluoride uptake by teeth. *Nuclear Instruments and Methods* 1981;**181**(1-3):327-31.
17. Balter V, Reynard B. Secondary ionization mass spectrometry imaging of dilute stable strontium labeling in dentin and enamel. *Bone* 2008;**42**(1):229-34.
18. Brudevold F, Reda A, Aasenden R, Bakhos Y. Determination of trace elements in surface enamel of human teeth by a new biopsy procedure. *Archives of Oral Biology* 1975;**20**(10):667-73.
19. Webb E, Amarasiriwardena D, Tauch S, Green EF, Jones J, Goodman AH. Inductively coupled plasma-mass (ICP-MS) and atomic emission spectrometry (ICP-AES): Versatile analytical techniques to identify the archived elemental information in human teeth. *Microchemical Journal* 2005;**81**(2):201-08.
20. McRae R, Bagchi P, Sumalekshmy S, Fahrni CJ. In Situ Imaging of Metals in Cells and Tissues. *Chemical Reviews* 2009;**109**(10):4780-827.
21. Hare D, Reedy B, Grimm R, Wilkins S, Volitakis I, George J, Cherny RA, Bush AI, Finkelstein DI, Doble P. Quantitative elemental bio-imaging of Mn, Fe, Cu and Zn in 6-hydroxydopamine Parkinsonism mouse models. *Metallomics* 2009;**1**:53.
22. Austin C, Hare D, Rozelle AR, Robinson WH, Grimm R, Doble P. Elemental bio-imaging of calcium phosphate crystal despoits in knee samples from arthritic patients. *Metallomics* 2009;**1**:142-47.
23. Hare D, Tolmachev S, James A, Bishop D, Austin C, Fryer F, Doble P. Elemental Bio-imaging of Thorium, Uranium, and Plutonium in Tissues from Occupationally Exposed Former Nuclear Workers. *Analytical Chemistry* 2010;**82**(8):3176-82.
24. Hare D, Burger F, Austin C, Fryer F, Grimm R, Reedy B, Scolyer Richard A, Thompson John F, Doble P. Elemental bio-imaging of melanoma in lymph node biopsies. *The Analyst* 2009;**134**:450-53.
25. Hoffmann E, Stephanowitz H, Ullrich E, Skole J, Ludke C, Hoffmann B. Investigation of mercury migration in human teeth using spatially resolved analysis by laser ablation-ICP-MS. *Journal of Analytical Atomic Spectrometry* 2000;**15**(6):663-67.
26. Kang D, Amarasiriwardena D, Goodman AH. Application of laser ablation-inductively coupled plasma-mass spectrometry (LA-ICP-MS) to investigate trace metal spatial distributions in human tooth enamel and dentine growth layers and pulp. *Analytical and Bioanalytical Chemistry* 2004;**378**(6):1608-15.
27. Arora M, Hare D, Austin C, Smith DR, Doble P. Spatial distribution of manganese in enamel and coronal dentine of human primary teeth. *Science of the Total Environment* 2011;**409**(7):1315-19.
28. Certificate of Analysis, Standard Reference Material (Bone Meal). 1992 [cited Jan 19, 2011]; Available from: https://www-s.nist.gov/srmors/view_cert.cfm?srm=1486
29. Zaichick V, Ovchjarenko N, Zaichick S. In vivo energy dispersive X-ray fluorescence for measuring the content of essential and toxic trace elements in teeth. *Applied Radiation and Isotopes* 1999;**50**(2):283-93.
30. Humphrey LT, Dean MC, Jeffries TE, Penn M. Unlocking evidence of early diet from tooth enamel. *Proceedings of the National Academy of Sciences of the United States of America* 2008;**105**(19):6834-39.
31. Tvinnereim HM, Eide R, Riise T, Fosse G, Wesenberg GR. Zinc in primary teeth from children in Norway. *The Science of The Total Environment* 1999;**226**(2-3):201-12.
32. Arora M, Kennedy BJ, Elhlou S, Pearson NJ, Walker DM, Bayl P, Chan SWY. Spatial distribution of lead in human primary teeth as a biomarker of pre- and neonatal lead exposure. *Science of the Total Environment* 2006;**371**(1-3):55-62.
33. Arora M, Y. Chan SW, Kennedy BJ, Sharma A, Crisante D, Murray Walker D. Spatial distribution of lead in the roots of human primary teeth. *Journal of Trace Elements in Medicine and Biology* 2004;**18**(2):135-39.
34. Arruda-Neto JDT, Geraldo LP, Prado GR, Garcia F, Bittencourt-Oliveira MC, Sarkis JES, Martinez-Lusardo F, Lima-Cazorla L, Rosa-Medero D, Rodrigues TE, Genofre GC. Study of metals transfer from environment using teeth as biomonitor. *Environment International* 2010;**36**(3):243-46.

35. Tibi M, Heumann KG. Isotope dilution mass spectrometry as a calibration method for the analysis of trace elements in powder samples by LA-ICP-MS. *Journal of Analytical Atomic Spectrometry* 2003;**18**(9):1076-81.